Proteins Lamin A and SUN1 are exclusively decreased in nuclear grade 4 clear cell renal cell carcinoma

RIO SHIBANUMA[1], SAYAKA KOBAYASHI[1], MOMOKA KONNO[1], RIO KANEKO[1], YOSHIMI NISHIJIMA[1], HAYATO IKOTA[2], MASASHI NOMURA[3], KAZUHIRO SUZUKI[3], HIDEAKI YOKOO[4] and MASANAO SAIO[1]

[1]Laboratory of Histopathology and Cytopathology, Department of Laboratory Sciences, Gunma University Graduate School of Health Sciences, Maebashi, Gunma 371-8514, Japan; [2]Clinical Department of Pathology, Gunma University Hospital, Maebashi, Gunma 371-8511, Japan; [3]Department of Urology, Gunma University Graduate School of Medicine, Maebashi, Gunma 371-8511, Japan; [4]Department of Human Pathology, Gunma University Graduate School of Medicine, Maebashi, Gunma 371-8511, Japan

Received October 1, 2025; Accepted November 4, 2025

DOI: 10.3892/ol.2025.15439

Abstract. Clear cell renal cell carcinoma (ccRCC) nuclear grade is associated with patient prognosis. Currently, the World Health Organization (WHO)/International Society of Urologic Pathologists (ISUP) grading system is used to evaluate nuclear and cellular morphology. The present study aimed to investigate the relationship between nuclear envelope-associated protein expression and nuclear grade. A total of 199 patients diagnosed with ccRCC were included in the study. Following immunohistochemical staining for Lamin A, Lamin B1, Lamin B2, Emerin, SUN1, SUN2, Nesprin-1, Nesprin-2 and Nesprin-3, their expression levels were evaluated. Comparing the nuclear grade with the mean nuclear area and perimeter revealed a significant increase across each grade from G1 to G3. However, the difference between G3 and G4 was not significant, indicating that nuclear morphology in G4 may be influenced by another factor. Comparison of Lamin expression across nuclear grades showed that only Lamin A was significantly decreased in G4 cases. Furthermore, the positive rates of Lamin B1 and Lamin B2, as well as nuclear grade, did not differ significantly between the grades. Next, the association between changes in Emerin, SUN and Nesprin expression and nuclear grade was examined; notably, only SUN1 showed significant changes in G4, whereas no significant differences were observed between nuclear grade and the other proteins. Therefore, reduced Lamin A and SUN1 expression may cause morphological changes in the nucleus and cells, leading to a shift toward G4. The total volumes of the nucleus and nucleoli showed an isometric relationship. Thus, evaluating the nucleolus using nuclear grade classification in G1-G3 ccRCC is essentially equivalent to evaluating the size of the nucleus. In conclusion, in the WHO/ISUP grading system, G1, G2 and G3 rely solely on nucleolar size as an indicator. However, in G4, both nuclear and cell morphology may be considered as indicators, since changes in nuclear envelope-associated proteins were only detected in this grade.

Correspondence to: Professor Masanao Saio, Laboratory of Histopathology and Cytopathology, Department of Laboratory Sciences, Gunma University Graduate School of Health Sciences, 39-22 3-chome, Showa-machi, Maebashi, Gunma 371-8514, Japan
E-mail: saio@gunma-u.ac.jp

Key words: clear cell renal cell carcinoma, Lamin, SUN, World Health Organization/International Society of Urologic Pathologists grading system, Fuhrman grade

Introduction

According to the latest cancer statistics from the International Agency for Research on Cancer, 434,419 new cases and 155,702 deaths from renal cancer were reported in 2022 (1). Renal cell carcinoma (RCC) includes histological subtypes such as clear cell RCC (ccRCC), papillary RCC, and chromophobe RCC (2). Among these, ccRCC represents the highest proportion, accounting for 70-75% of all RCCs (2). Compared with non-ccRCC, ccRCC is associated with higher mortality and lower survival rates, indicating the poorest prognosis among RCCs (2,3). Furthermore, ccRCC originates from proximal tubule epithelial cells and typically exhibits an expansive growth pattern (4). Histologically, it is marked by abundant clear cytoplasm resulting from lipid and glycogen accumulation (2). The Fuhrman grade (5) and the WHO/ISUP grading system (6) are generally used to grade the nuclear features of ccRCC. Higher nuclear grades correlate with poorer prognosis; therefore, these nuclear grading systems have been used in clinical practice. However, recent studies have indicated that the Fuhrman grade has moderate interobserver agreement (7). Because of subjectivity in how pathologists emphasize specific criteria and assess nuclear size, it has been suggested that grading beyond Grade 4 should primarily focus on nucleolar evaluation (7,8). Dagher *et al* (8) suggested that the WHO/ISUP grading system correlates more strongly with patient survival than the Fuhrman grade.

Changes in nuclear morphology are reported to be influenced by changes in the expression of nuclear envelope (NE)-associated proteins, including Lamin, Emerin, SUN, and Nesprin (9). In particular, Lamins are classified into two types: A-type and B-type Lamin (10). Lamin A, which

is on the nucleoplasmic side, forms a dense meshwork (10). Lamin B1, which is situated between Lamin A and the inner nuclear membrane (INM), forms a relatively loose meshwork (10). Lamin B1 prevents nuclear bleb formation caused by Lamin A protrusions (10). Lamin influences nuclear and cellular morphologies. Vahabikashi *et al* (11) reported that Lamin A deficiency leads to nuclear distortion and increased nuclear volume, whereas Lamin B1 or B2 deficiency causes no evident distortion. In Lamin B1-deficient cells, nuclear volume is smaller than in wild-type cells, whereas in Lamin B2 deficiency, it is nearly identical to wild-type. Furthermore, Lamin interacts with the Linker of Nucleoskeleton and Cytoskeleton (LINC) complex and intermediate filaments, thereby regulating cytoplasmic stiffness (11). The effects of Lamin also vary by tumor type. Moss *et al* (12) reported that in esophageal squamous cell carcinoma, Lamin A/C is reduced while Lamin B1 is retained, whereas in colon tumors and gastric dysplasia, both Lamin A/C and B1 are decreased. Conversely, pancreatic cancer retains the expression of both Lamin proteins (12). Although reduced Lamin expression is common in cancer, it is not observed in all epithelial tumors (12). Previous studies have also reported findings related to Emerin (13,14). Vaughan *et al* (14) reported that Lamin A, C, and B1 interact with Emerin; when Lamin A/C is absent from the NE, Emerin relocates from the NE to the endoplasmic reticulum. Hence, Lamin A is necessary to anchor Emerin to the NE. Lammerding *et al* (13) reported that Emerin deficiency induces abnormalities in the nuclear shape; however, these are milder than those caused by Lamin A deficiency, and nuclear rigidity remains comparable to that of wild type. Furthermore, SUN and Nesprin interact with both Lamin and Emerin as well as the cytoskeleton, thereby influencing both the nucleoskeleton and cytoskeleton (15,16). Haque *et al* reported that the C-terminals of SUN1 and SUN2 interact with the KASH domains of Nesprin-1 and -2, linking the nucleus to actin, whereas their N-terminals interact with nuclear Lamin, Emerin, and short Nesprin-2 isoforms. These interactions bridge the nucleoskeleton and the cytoskeleton, playing a crucial role in maintaining nuclear and cellular integrity (15). Banerjee *et al* (17) reported that deficiency of either Nesprin-1 or Nesprin-2 increases nuclear area and perimeter and reduces roundness; when both are deficient, the localization of Lamin A/C and Emerin is disrupted. Ketema *et al* (16) demonstrated that Nesprin-3, similar to Nesprin-1 and -2, localizes to the outer nuclear membrane through interactions with SUN1 and SUN2. Furthermore, Nesprin-3α binds to plectin dimers, linking intermediate filaments to the nucleus, whereas the interaction between SUN and Lamin A forms the Nesprin-3-LINC complex that bridges the cytoskeleton and nucleoskeleton (16). Heffler *et al* (18) also reported that Nesprin-3 deficiency increases the number of nuclear wrinkles and indentations.

Several studies have reported the contribution of altered expression levels of Lamin, Emerin, SUN, and Nesprin to nuclear and cellular morphologies. Therefore, examining the expression of these NE-associated proteins may help identify potential indicators of nuclear grade. Regarding kidney cancer, Xin *et al* reported that reduced Lamin A expression contributes to abnormal nuclear morphology (19). Radspieler *et al* (20) also reported that the gene expression levels of Lamin B1 serve as a marker of poor prognosis. Furthermore, Fukushima *et al* (21) demonstrated that reduced Nesprin-1 gene expression is a poor prognostic factor and that its knockdown enhances invasive potential. However, to our knowledge, no studies have directly compared nuclear grade with the expression of NE-associated proteins to elucidate the mechanisms underlying nuclear morphological changes in ccRCC. Therefore, we conducted this study to investigate the relationship between nuclear grade and nine NE-associated proteins: Lamin A, Lamin B1, Lamin B2, Emerin, SUN1, SUN2, Nesprin-1, Nesprin-2, and Nesprin-3, which have been implicated in alterations of nuclear and cellular morphology.

Materials and methods

Samples. This study included 199 patients who underwent surgical resection for ccRCC at Gunma University Hospital between January 2005 and July 2012. The Gunma University Ethical Review Board for Medical Research Involving Human Subjects approved this study (approval no. HS2024-068). We used formalin-fixed and paraffin-embedded tissue blocks used for routine pathological diagnosis. Sections were cut at 4 μm thickness for immunohistochemical staining.

Evaluation of nuclear grade. Hematoxylin-eosin-stained diagnostic specimens, stored in the Department of Pathology at Gunma University Hospital, were reviewed by pathologists. The nuclear grades of four patient groups (G1-G4) were determined according to the Fuhrman grade (5) and WHO/ISUP grading systems (6).

Immunohistochemical staining. Four micrometer-thick sections were deparaffinized through three 5-min xylene treatments. For rehydration, sections were sequentially immersed in 100, 99, 95, and 70% ethanol for 1 min each, followed by a 1-min rinse under running water. For immunohistochemical staining, the following antibodies were used at a concentration of 2 μg/ml: anti-Lamin A antibody (clone 133A2; mouse monoclonal antibody; ab8980; Abcam), anti-Lamin B1 antibody (clone 3C10G12; mouse monoclonal antibody; 66095-1-Ig; Proteintech, Rosemont, USA), anti-Lamin B2 antibody (clone GT144; mouse monoclonal antibody; GTX628803; GeneTex, California, USA), anti-Emerin antibody (clone CL0201; mouse monoclonal antibody; NBP2-52876; Novus Biologicals, Centennial, CO, USA), anti-SUN1 antibody (clone EPR6554; rabbit monoclonal antibody; ab124770; Abcam), anti-SUN2 antibody (clone EPR6557; rabbit monoclonal antibody; ab124916; Abcam), anti-Nesprin-1 antibody (clone EPR14196; rabbit monoclonal antibody; ab192234; Abcam), anti-Nesprin-2 antibody (clone EPR28137-54; rabbit monoclonal antibody; ab186746; Abcam), and anti-Nesprin-3 antibody (clone EPR15623; rabbit monoclonal antibody; ab314872; Abcam). First, sections were placed in an electric pot containing Immunosaver (Nisshin EM Co. Ltd., Shinjuku-ku, Tokyo, Japan) diluted 200-fold with distilled water for antigen retrieval. Next, they were boiled, maintained at 98˚C for 40 min, and left in the pot for 30 min after turning off the heat. Subsequently, they were transferred to a container with 0.01 M phosphate-buffered saline (PBS) solution. Following antigen retrieval, immunohistochemical

staining was performed using an automated staining system (Histostainer 36A; Nichirei Biosciences, Chuo-ku, Tokyo, Japan). We treated the specimens with hydrogen peroxide solution (code 715242; Nichirei Bioscience) for 5 min to block endogenous peroxidase activity. After the specimens were washed with PBS (code 715224; Nichirei Bioscience), 2% goat serum (ab7481; Abcam) was added and incubated for 15 min. Primary antibodies (clones 133A2, 3C10G12, GT144, CL0201, EPR6554, EPR6557, EPR14196, EPR28137-54, and EPR15623) were applied and incubated at room temperature for 60 min. After washing, peroxidase-labeled anti-mouse IgG polyclonal antibody (Histofine Simple Stain MAX-PO(M); code 724132; Nichirei Bioscience) was applied as the secondary antibody for 30 min to specimens treated with primary antibodies, including clones 133A2, 3C10G12, GT144, and CL0201. For clones EPR6554, EPR6557, EPR14196, EPR28137-54, and EPR15623, peroxidase-labeled anti-rabbit IgG polyclonal antibody (Histofine Simple Stain MAX-PO(R); code 724142; Nichirei Bioscience) was used as the secondary antibody for 30 min. For color development, the specimens were incubated with the DAB substrate kit (code 725191; Nichirei Bioscience) twice for 10 min. After washing, the nucleus was stained with hematoxylin (code 715081; Nichirei Bioscience) for 1 min. Subsequently, the specimens were removed from the automatic staining machine and washed once with distilled water. Next, sections were dehydrated in 70, 95, and 100% ethanol (two baths) for 1 min each. For clearing, xylene was applied in three consecutive baths for 5 min, followed by mounting. Subsequently, the sections were examined using an optical microscope (BX51; Evident, Tokyo, Japan) to confirm staining.

Acquisition of specimen images using a virtual slide scanner. Whole-slide images of immunohistochemically stained specimens for Lamin A, B1, and B2 were obtained using a virtual slide scanner (Nano Zoomer 2.0-HT Virtual Slide Scanner; C9600-13; Hamamatsu Photonics K.K., Shizuoka, Japan). The scanning conditions were as follows: observation lens, 20x; resolution, 0.75; scan mode, 40x; maximum capture size, 26x76 mm; pixel size, 0.23 μm/pixel; light source, halogen lamp; and image storage format, JPEG.

Computer-assisted image analysis. For analyzing Lamin A-, B1-, and B2-stained specimens, five representative regions per specimen were selected at 40x magnification from whole-slide images and saved as TIFF files. The images were then analyzed using the NE measurement software e-Nucmen3 (ver. 1.8; E-path Co. Ltd, Fujisawa, Kanagawa, Japan). To focus on tumor cell nuclei, nontumor regions were excluded using the annotation function. Nuclei of nontumor cells within the tumor region, overlapping nuclei, and nuclei not correctly recognized by the software were also excluded. Analysis conditions are provided in Table SI.

Evaluation of Emerin, SUN, and Nesprin expression. Specimens stained with each primary antibody were examined under a microscope. To evaluate expression changes, staining intensity in the tumor region was compared with that of the nuclear membrane in normal proximal tubules from the same patient. Expression levels of Emerin, SUN1, SUN2, and Nesprin-2 were classified into three categories: decreased, no change, and increased. For Nesprin-1, the expression level was classified into decreased, no change, and nucleoplasm. For Nesprin-3, because no expression was detected in the NE of normal proximal tubules, expression was classified as no change (absent) or increased (present).

Statistical analysis. All statistical data were analyzed using JMP Pro ver. 18. 2.0 (SAS Japan, Tokyo, Japan). For multiple comparisons involving unequal group sample sizes (unbalanced data), one-way ANOVA was initially performed to check variance among groups, after which, the Tukey-Kramer HSD test was used for pair-wise comparisons, referencing Lee and Lee (22) for its validity. Because part of the statistical evaluation involved qualitative assessment, Fisher's exact test was used for 2x2 group comparisons to examine the presence or absence of distribution differences (23). Comparisons involving more than two groups were analyzed using the Fisher-Freeman-Halton exact conditional test (24). Association between two continuous variables were assessed using linear regression analysis. Association strength was classified according to the correlation coefficient (r) as follows: 0.200-0.399, weak; 0.400-0.699, moderate; and ≥0.700, strong. $P<0.05$ was considered to indicate a statistically significant difference (25).

Results

Nuclear size increased from G1 to G3. Table I summarizes the clinicopathological characteristics of the patients (26). First, the mean nuclear area and perimeter were compared with Fuhrman and WHO/ISUP grades. G1-G3 showed a significant increase in mean nuclear area and perimeter across both grading systems. However, neither grading system showed a significant difference between G3 and G4 (Fig. 1A-D). Therefore, nuclear size may not adequately represent G4, and other factors likely contribute to nuclear and cellular morphology in this grade. The representative G1 to G4 grade histological images of HE staining for both Fuhrman and WHO/ISUP grades are shown in Fig. S1.

Decreased Lamin A expression influences nuclear shape changes in G4. Next, we examined the positive rates for Lamin A, B1, and B2 according to the two grading systems. Mean Lamin A positive rates by grade were 63.4, 65.2, 68, and 42.6% for G1, G2, G3, and G4 in the Fuhrman grade and 63.4, 65.9, 66.3, and 42.6% in the WHO/ISUP grading system, respectively. Thus, the Lamin A positive rate was significantly lower in G4 than in G1-G3 in both grading systems (Fig. 2A and B). Meanwhile, the mean Lamin B1 positive rates were 31.1, 32.8, 34.4, and 34.9% for G1, G2, G3, and G4 cases in Fuhrman grade and 32.4, 33.7, 32.5, and 34.9% in the WHO/ISUP grading system, respectively. For Lamin B2, mean positive rates by grade were 70.1, 74, 73, and 67.9% for G1, G2, G3, and G4 in the Fuhrman grade and 72.3, 74.7, 71.7, and 67.9% in the WHO/ISUP grading system, respectively. Positive rates of Lamin B1 or B2 did not differ significantly between groups in either grading systems (Fig. 2C-F). We compared the positive rates for each Lamin with the mean nuclear area, perimeter, and circularity. The positive rate for Lamin A showed no association with mean nuclear area or

Table I. Clinicopathological characteristics of patients.

Characteristic	Value
Total number of patients, n (%)	199 (100)
Mean age, years	63.0
Sex, n (%)	
Male	142 (71)
Female	57 (29)
Fuhrman grade, n (%)	
1	10 (5)
2	117 (59)
3	59 (30)
4	13 (6)
WHO/ISUP grading system, n (%)	
1	8 (4)
2	109 (55)
3	69 (35)
4	13 (6)
pT status, n (%)	
pT1	169 (85)
pT2	10 (5)
pT3	19 (10)
pT4	1 (0.5)
pN status, n (%)	
pN0	196 (85)
pN1	3 (15)
pM status, n (%)	
pM0	194 (97)
pM1	5 (3)
Stage, n (%)	
I	165 (83)
II	10 (5)
III	16 (8)
IV	8 (4)

perimeter (Fig. 3A and B) but exhibited a weak association with mean circularity (Fig. 3C). Furthermore, the positive rate for Lamin B1 did not associate with any of the nuclear shape indicators (Fig. 3D-F). The positive rate of Lamin B2 was not associated with the mean nuclear area or mean nuclear perimeter (Fig. 3G and H) but weakly associated with the mean circularity (Fig. 3I). Therefore, only Lamin A exhibited a significant decrease in expression in G4 cases. Furthermore, Lamin A and B2 were weakly associated with the maintenance of nuclear shape across all grades. The representative images of Lamin A, B1 and B2 based on the WHO/ISUP grading system was shown in Fig. S2.

SUN1 reduction in G4 cases correlates with nuclear grade. In addition to Lamin, we examined the association of expression changes in Emerin, SUN, and Nesprin with nuclear grade (Fig. 4A-L). In the Fisher-Freeman-Halton exact conditional test, Emerin showed a significant difference between groups in the Fuhrman grade (P=0.0488) but not in the WHO/ISUP grading system (P=0.0690) (Fig. 4Aand D). For SUN1, significant differences were observed between groups in both nuclear grading systems (P<0.0001) (Fig. 4B and E). Similarly, SUN2 showed significant between-group differences in the Fuhrman grade (P=0.0289) and the WHO/ISUP grading system (P=0.0143) (Fig. 4C and F). In contrast, Nesprin-1 and Nesprin-2 showed no significant changes between groups in either grading system (Fig. 4G, H, J and K). In all 199 cases, Nesprin-3 expression was negative in the nuclear membranes of normal proximal tubules and that of tumor cells (Fig. 4I and L). SUN1, which demonstrated the most significant changes, showed reduced expression was increased in G4 cases; in other grades, expression either increased or remained unchanged. Therefore, a Fisher's exact test was performed by dividing the cases into two groups: no change/increased vs. decreased, and G1-G3 vs. G4. The results revealed a significant reduction in SUN1 expression in G4 cases (Fig. 5A and B), suggesting that SUN1 reduction correlates with the progression of nuclear atypia to G4. Regarding the significant differences detected in Emerin and SUN2 expression by the Fisher-Freeman-Halton exact conditional test, the difference among groups would be exist. The representative image of SUN1 based on the WHO/ISUP grading system is shown in Fig. S3.

Discussion

In the WHO/ISUP grading system, G1-G3 are determined solely by nucleolar size, without reference to nuclear size or shape. In contrast, G4 is based on nuclear and cellular morphological changes, including marked nuclear atypia, multinucleated giant cells, sarcomatoid features, and rhabdoid changes (6). Because nuclear grade correlates with prognosis (8), investigating its underlying mechanisms is essential. Accordingly, in this study, we compared the expression of NE-associated proteins with nuclear grade. To our knowledge, no studies have compared nuclear grade with NE-associated protein expression to elucidate the mechanism of nuclear morphological changes in ccRCC. Capo-chichi *et al* (27) reported that many cells in cervical smear specimens negative for Lamin A/C contained enlarged, irregularly shaped nuclei. Furthermore, Xin *et al* (19) reported that knockdown of the *LMNA* gene encoding Lamin A in kidney cancer cell lines resulted in NE invaginations and abnormalities in nuclear contours. Therefore, we first investigated Lamin's contribution to nuclear grade, followed by an examination of the mechanisms underlying nuclear morphological changes in ccRCC. We found that Lamin A expression levels were reduced in G4 cases, whereas those of Lamin B1 and B2 showed no significant changes. Lammerding *et al* reported that in mouse embryonic fibroblasts, reduced Lamin A decreased nuclear stiffness, whereas Lamin B1 or B2 had no effect (28). Furthermore, although Lamin B1 reduction increased nuclear bleb formation, it did not alter overall nuclear rigidity or shape stability (28). In a study by Pujadas Liwag *et al* (29) using human colon adenocarcinoma cell lines, reduced B-type Laminincreased nuclear volume and nuclear bleb formation. Based on these findings, B-type Lamin contributes to nuclear bleb formation, but its effect on overall nuclear morphology is less pronounced

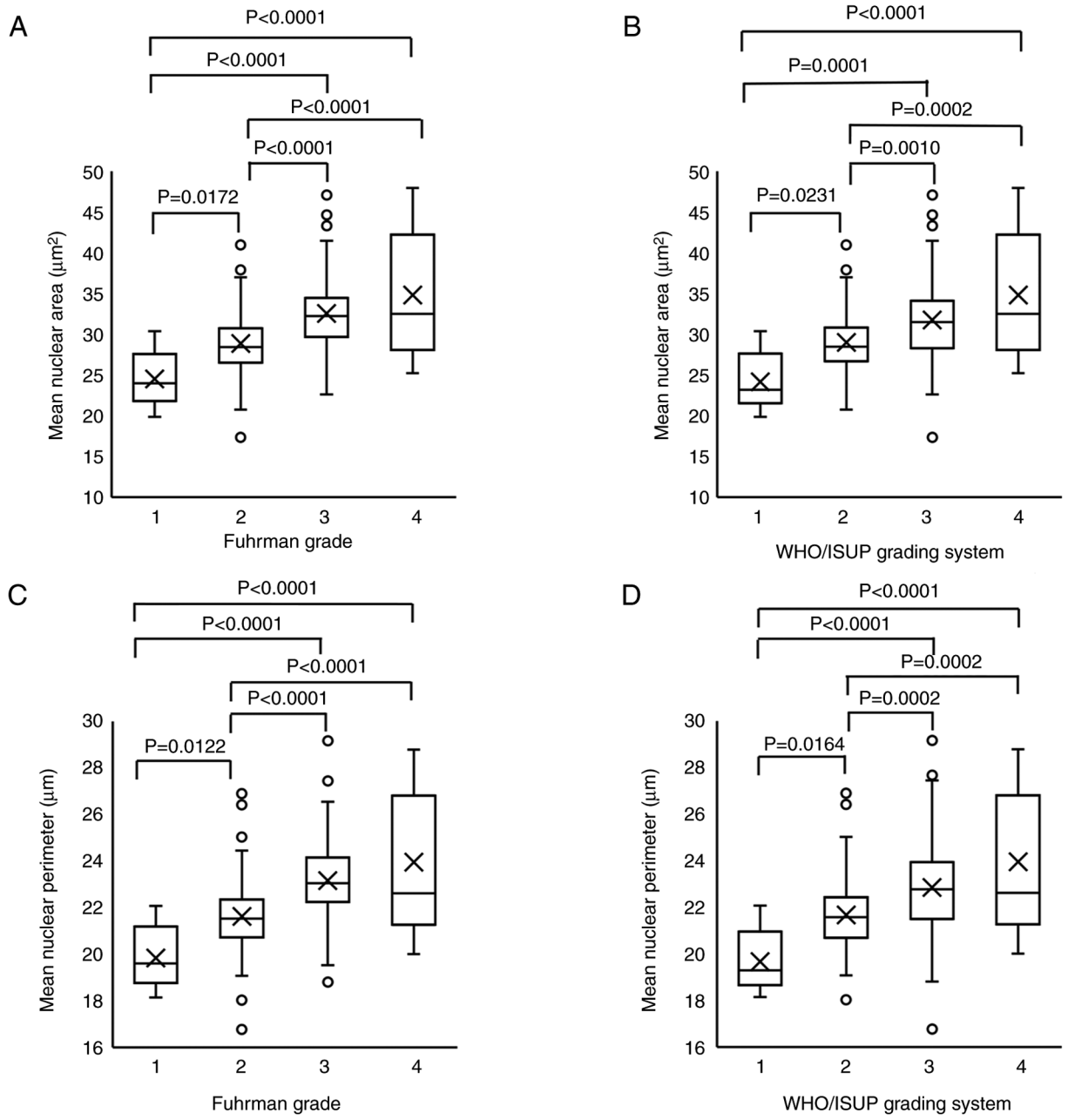

Figure 1. Comparison of nuclear size and nuclear grade. (A) Mean nuclear area vs. Fuhrman grade. (B) Mean nuclear area vs. the WHO/ISUP grading system. (C) Mean nuclear perimeter vs. Fuhrman grade. (D) Mean nuclear perimeter vs. the WHO/ISUP grading system. In the box-and-whisker plots, 'X' indicates the mean value; horizontal lines represent the median and interquartile range, and the whiskers denote the minimum and maximum values. P-values were calculated using the Tukey-Kramer HSD test. WHO, World Health Organization; ISUP, International Society of Urologic Pathologists; HSD, honest significant difference.

than that of Lamin A. Harborth *et al* (30) reported that silencing Lamin B1 and B2 in HeLa cells and rat fibroblasts induced growth arrest and apoptosis. These findings suggest that Lamin A is involved in maintaining nuclear morphology and Lamin B1 and Lamin B2 are involved in other functions, including cell proliferation. This interpretation does not appear to contradict the results of the present study.

Reis-Sobreiro *et al* (31) reported that Emerin deficiency leads to irregular nuclear shapes, reduced roundness, and impaired deformability in prostate and breast cancer cell lines. Furthermore, Lamin A/C downregulation contributes to nuclear shape instability and destabilization such as Emerin mislocalization (31). Based on this report, considering that Emerin may influence nuclear morphology, we investigated its effect on nuclear pleomorphism classification. In G4 nuclei, cellular morphological changes such as sarcomatoid and rhabdoid features are also considered indicators (6). NE-associated proteins such as SUN and Nesprin interact to form the LINC complex (32). Lombardi *et al* (33) reported that LINC complex disruption causes defects in nuclear positioning, cytoskeletal organization, and cell/nuclear deformation. The mechanisms underlying both nuclear and cellular morphological changes were investigated by examining the relationship between changes in SUN and Nesprin expression and nuclear grade. In this study, SUN1 expression decreased in G4 cases, similar to Lamin A. Emerin and SUN2 also showed significant intergroup

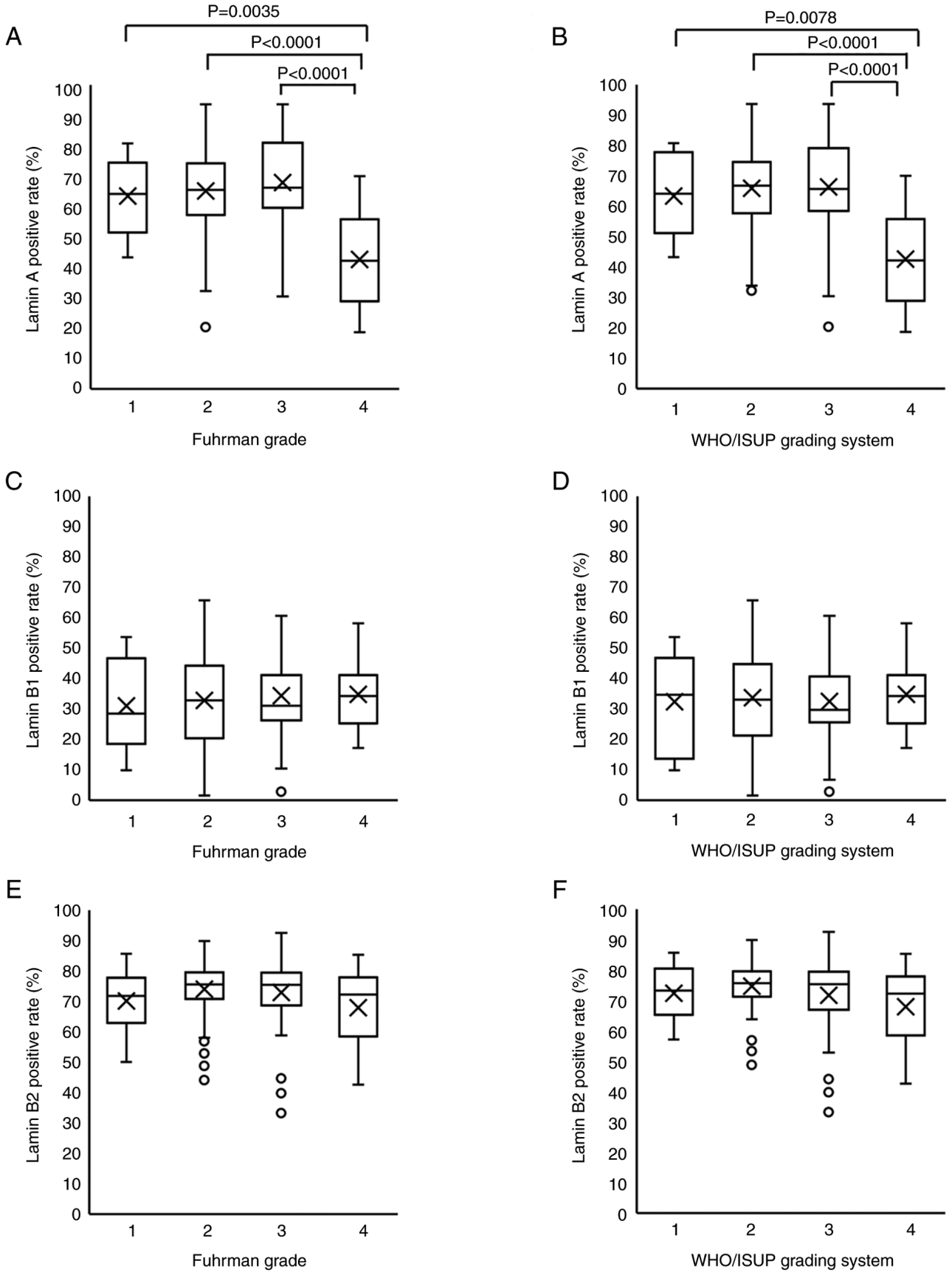

Figure 2. Comparison of Lamin positive rates and nuclear grade. (A) Lamin A positive rate (%) vs. Fuhrman grade. (B) Lamin A positive rate (%) vs. the WHO/ISUP grading system. (C) Lamin B1 positive rate (%) vs. Fuhrman grade. (D) Lamin B1 positive rate (%) vs. the WHO/ISUP grading system. (E) Lamin B2 positive rate (%) vs. Fuhrman grade. (F) Lamin B2 positive rate (%) vs. the WHO/ISUP grading system. In the box-and-whisker plots, 'X' indicates the mean value; horizontal lines represent the median and interquartile range, and whiskers denote the minimum and maximum values. P-values were calculated using the Tukey-Kramer HSD test. WHO, World Health Organization; ISUP, International Society of Urologic Pathologists; HSD, honest significant difference.

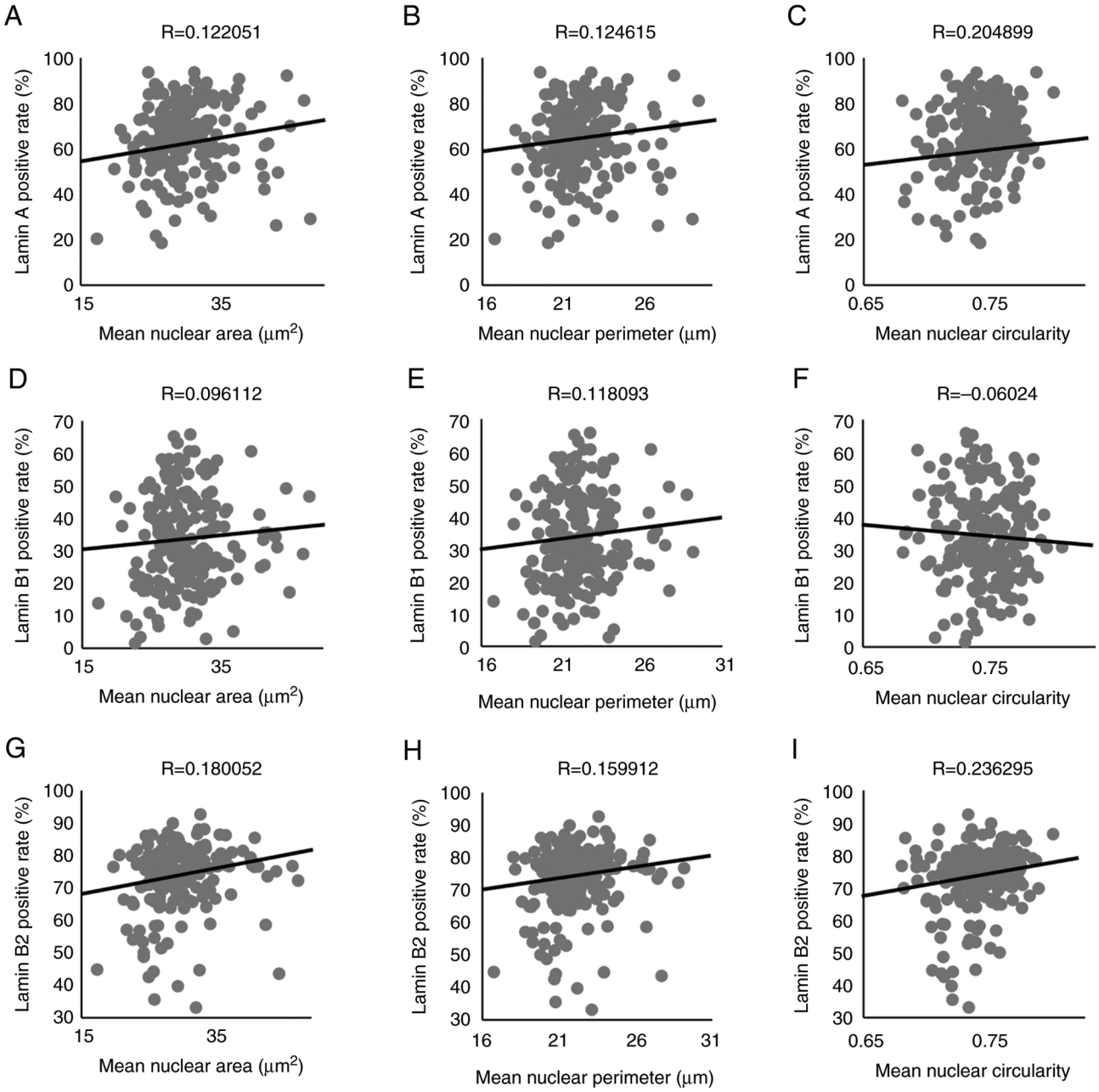

Figure 3. Comparison of Lamin positive rates and nuclear shape factors. (A-C) Lamin A positive rate vs. nuclear shape factors: (A) Mean nuclear area, (B) mean nuclear perimeter, (C) mean nuclear circularity. (D-F) Lamin B1 positive rate vs. nuclear shape factors: (D) Mean nuclear area, (E) mean nuclear perimeter, (F) mean nuclear circularity. (G-I) Lamin B2 positive rate vs. nuclear shape factors: (G) Mean nuclear area, (H) mean nuclear perimeter, (I) mean nuclear circularity. Straight lines in the graphs represent regression lines. The correlation coefficient (R) was calculated using linear regression analysis.

differences. Although the proportion of G1 cases with reduced Emerin expression was higher than in other grades, the difference was statistically significant only in the Fuhrman grade, not in the WHO/ISUP classification. Therefore, the small number of G1 cases may have influenced the observed significance. For SUN2, between-group differences were significant in the Fuhrman grade and the WHO/ISUP grading system, although they looked unclear in Fig. 4E and F. Thus, despite the possibility of differences in Emerin and SUN2 among groups, describing a specific association between nuclear grade and protein expression changes in ccRCC was difficult in this study. For Nesprin-1, Nesprin-2, or Nesprin-3, the changes were not significant in relation to nuclear grade. Matsumoto *et al* (34) reported that in breast cancer specimens, Lamin A, SUN1, SUN2, and Nesprin-2 expression was downregulated in cancerous areas compared with that in noncancerous ones. Accordingly, their findings for SUN2 and Nesprin-2 do not align with our results, possibly caused by organ-specific differences. Ueda *et al* (35) reported that SUN1 deficiency in HeLa cells, with no actin reduction observed in SUN2-deficient cells led to reduced actin, decreased cytoskeletal force, and diminished contractile force, whereas SUN2 deficiency had no effect on actin, indicating a specific role for SUN1 in cytoskeletal regulation (35). Therefore, SUN1 deficiency may contribute to reduced tumor differentiation. The observed reduction of SUN1 expression in G4 cases in our

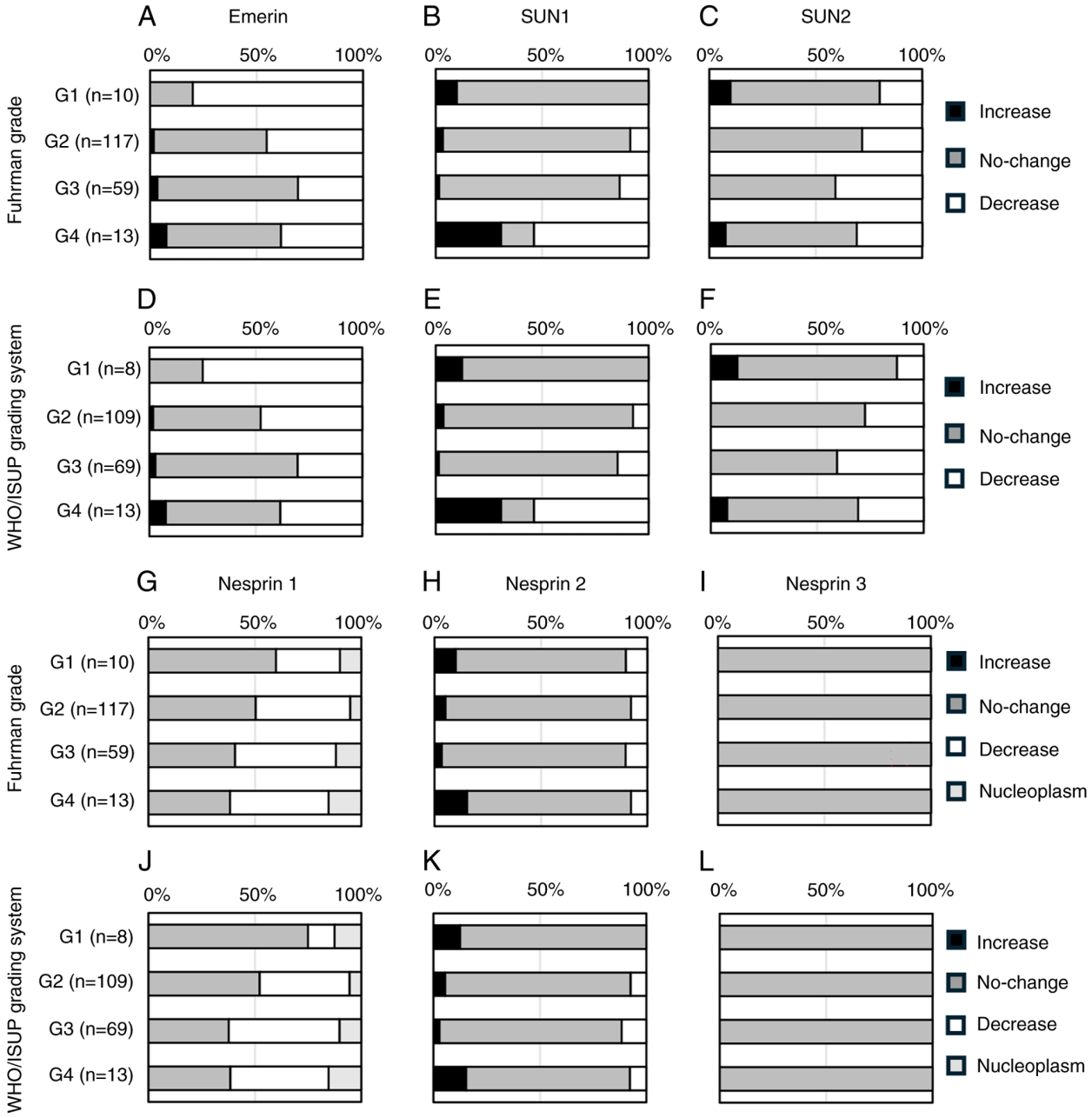

Figure 4. Comparison of nuclear envelope-associated protein expression and nuclear grade. (A) Emerin expression vs. Fuhrman grade, (B) SUN1 expression vs. Fuhrman grade, (C) SUN2 expression vs. Fuhrman grade. (D) Emerin expression vs. WHO/ISUP grading system, (E) SUN1 expression vs. WHO/ISUP grading system, (F) SUN2 expression vs. WHO/ISUP grading system. (G) Nesprin1 expression vs. Fuhrman grade, (H) Nesprin2 expression vs. Fuhrman grade, (I) Nesprin3 expression vs. Fuhrman grade. (J) Nesprin1 expression vs. WHO/ISUP grading system, (K) Nesprin2 expression vs. WHO/ISUP grading system, (L) Nesprin3 expression vs. WHO/ISUP grading system. WHO, World Health Organization; ISUP, International Society of Urologic Pathologists.

study is consistent with the findings of Ueda *et al* (35). In our study, SUN1 was reduced only in G4 cases, similar to Lamin A; thus, Lamin A may be related to SUN1. Östlund *et al* (36) demonstrated that Lamin A is more closely associated with SUN1 than with SUN2. Haque *et al* (37) reported that although SUN1 interacts with Lamin A, it localizes to the NE even in the absence of Lamin A, indicating that Lamin A is not required for the NE localization of SUN1. Nishioka *et al* (38) reported that SUN1 interacts with Lamin B1 and B2, whereas SUN2 shows no interaction with B-type Lamin. Therefore, SUN1 may be associated with Lamin A, B1, and B2. However, the present results suggest that only Lamin A is associated with SUN1 in ccRCC. Sharma *et al* (39) reported that SUN1/2 knockdown in rat mammary carcinoma cell lines caused irregular nuclear morphology. As Lamin expression and localization remained unchanged, the nuclear defects of SUN1/2 were not attributable to off-target effects on Lamin. In our study, both Lamin A and SUN1 expression were reduced in G4 cases. These findings suggest that Lamin A and SUN1 are interrelated or independently contribute to nuclear morphological alterations. Considering that Nesprin-1 was expressed in the nucleoplasm, we examined the basis for this localization pattern. Mislow *et al* (40) reported that Nesprin-1α can bind both Lamin and Emerin, acting as a structural cross-linker

A

Protein	Protein expression	Fuhrman grade		
		G1-G3	G4	Total
Nuclear membrane expression of SUN1	Increase/No-change	168	6	174
	Decrease	18	7	25
	Total	186	13	199

As determined by Fisher's exact test, there was a significant difference among groups : P=0.0002.

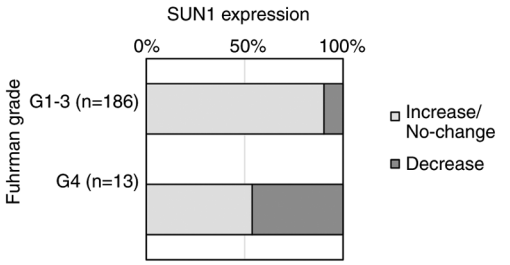

B

Protein	Protein expression	WHO/ISUP grading system		
		G1-G3	G4	Total
Nuclear membrane expression of SUN1	Increase/No-change	168	6	174
	Decrease	18	7	25
	Total	186	13	199

As determined by Fisher's exact test, there was a significant difference among groups : P=0.0002.

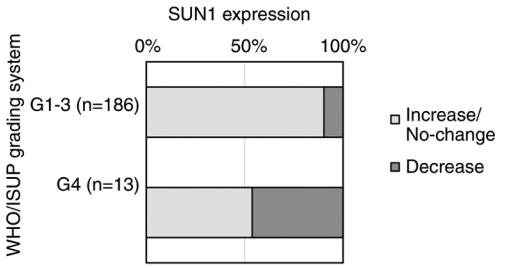

Figure 5. Comparison of SUN1 expression and nuclear grade. (A) SUN1 expression vs. Fuhrman grade. (B) SUN1 expression vs. WHO/ISUP grading system. WHO, World Health Organization; ISUP, International Society of Urologic Pathologists.

that anchors these proteins to the INM. Duong *et al* (41) reported that Nesprin-1α-1 was undetectable at very low levels in all tissues, whereas Nesprin-1α and -2 were highly expressed exclusively in cardiac and skeletal muscles. The proportions of the Nesprin isoforms Nesprin-2-Giant and Nesprin-1-Giant in the kidney were 81 and 15%, respectively (41). Furthermore, in cells lacking the KASH domain of Nesprin-2, this protein exhibited a speckled pattern within the nucleoplasm (41). Therefore, the nucleoplasmic staining of Nesprin-1 observed in this study may reflect the absence of the KASH domain, considering the very low levels of Nesprin-1α in the kidney. Moreover, Sur-Erdem *et al* (42) reported that Nesprin-1 overexpression restored abnormalities in tumor cell nuclear structure, NE organization, centrosome positioning, and genomic instability. Nesprin-1 interacts with Lamin and SUN proteins, contributing to the maintenance of nuclear structure and cytoskeletal organization (42). However, we found no significant correlation between Nesprin-1 expression changes and nuclear grade, suggesting that Nesprin-1 slightly influences ccRCC. Furthermore, Nesprin-3 was negative in all cases, indicating that it was not associated with nuclear grade. Wilhelmsen *et al* (43) showed that Nesprin-3 binds to intermediate filaments via plectin. Morgan *et al* (44) reported that silencing Nesprin-3 induces cell elongation in human aortic endothelial cells. This was accompanied by a marked reduction in the nuclear periphery localization of plectin and the cytoskeletal protein vimentin, highlighting the importance of Nesprin-3 in maintaining the cytoskeletal structure of the nuclear periphery (44). However, our study showed that in the kidney, Nesprin-3 expression was detected only in stromal components, including mesangial cells and fibroblasts, but was absent in the ccRCC regions derived from the proximal tubules, similar to normal proximal tubules. Collectively, these findings suggest that Nesprin-3 has no role in ccRCC.

Next, we discuss the rationale for using only nuclear and cellular morphological characteristics to classify G4 in the WHO/ISUP grading system, whereas G1-G3 are defined primarily by the nucleolar size. In this study, the mean nuclear area and perimeter significantly increased with higher grades from G1 to G3 in both grading systems, whereas no significant differences were observed between G3 and G4. Therefore, factors different from those affecting G1-G3 may influence the transition to G4. In this study, comparison of NE-associated proteins with nuclear grade revealed that only Lamin A and SUN1 showed significantly reduced expression in G4. Thus, decreased Lamin A and SUN1 expression may contribute to nuclear and cellular morphological alterations associated with progression to G4. Diegmiller *et al* (45) reported that the total nuclear volume and total nucleolar volume in nurse cells exhibit a linear proportional relationship. Therefore, observing nucleolar size can be considered equivalent to observing nuclear size. In other words, our finding that nuclear size increases with grade from G1 to G3 likely reflects proportional changes between nucleolar and nuclear sizes. Conversely, our results indicate that G4 relies on nuclear and cellular morphology as diagnostic indicators, as alterations in NE-associated proteins such as Lamin A and SUN1 are observed only at this stage.

Although this study did not evaluate prognostic or therapeutic applications, we considered the potential diagnostic and therapeutic implications of Lamin A and SUN1 based on previous reports. Chiarini *et al* (46) reported that Lamin A functions as a tumor suppressor in Ewing sarcoma, where its introduction reduces invasive potential and high expression correlates with improved 5-year survival rates. Therefore, in ccRCC, reintroducing Lamin A in patients with reduced tumor cell Lamin A expression may improve survival outcomes. Regarding SUN, existing reports are primarily related to SUN2. In lung cancer, SUN2 suppresses cell proliferation and migration, and its overexpression enhances chemotherapy sensitivity (47). In contrast, low SUN2 expression is associated with shorter survival times (47). Although no studies have examined treatment or survival outcomes related to SUN1, Nishioka *et al* (38) reported that SUN1 promotes cell migration when overexpressed. Collectively, these findings suggest that SUN2 upregulation and SUN1 inhibition may have therapeutic potential. However, neither has been studied in ccRCC, indicating that this topic warrants future investigation.

Finally, this study has several limitations. First, the numbers of G1 and G4 cases were small, each accounting for approximately 5 and 6% of the 199 cases, respectively. Therefore, a larger cohort and more detailed analyses are necessary. Second, although Lamin expression was

quantitatively evaluated through image analysis, Emerin, SUN, and Nesprin expression relied on manual evaluation, potentially limiting analytical precision. Some proteins exhibited nucleoplasmic or cytoplasmic staining, resulting in varied patterns that could not be measured using the e-Nucmen3 nuclear membrane analysis software. Therefore, future research should focus on developing advanced analytical tools capable of handling diverse staining patterns to enable automated image-based quantification. Third, the study analyzed only human samples, providing limited evidence that reduced the expression of Lamin A or SUN1 directly causes changes in nuclear morphology. Therefore, cell or animal models should be used in future research to verify the underlying mechanisms.

In conclusion, in ccRCC, alterations in NE-associated protein expression were observed exclusively in G4 cases. Among Lamin, Emerin, SUN, and Nesprin proteins, only Lamin A and SUN1 showed altered expression. Although the nuclear for G1-G3 is determined based on the nucleolar size, this parameter also indirectly reflects nuclear size in image analysis. Notably, the influence of NE-associated proteins appears confined to G4 tumors. These findings provide important insight into why the WHO/ISUP grading system exclusively employs nuclear and cellular morphological features for G4 assessment.

Acknowledgements

Not applicable.

Funding

No funding was received.

Availability of data and materials

The data generated in the present study may be requested from the corresponding author.

Authors' contributions

RS collected clinicopathological data, and contributed to sectioning, immunohistochemistry, staining evaluation, image and statistical analyses, and manuscript preparation. MS planned and conducted the experiments, performed histological diagnosis of carcinoma cases, and performed image analysis, staining evaluation, statistical analysis and manuscript preparation. SK performed immunohistochemistry, conducted image analysis and reviewed the literature. YN performed whole-slide imaging and reviewed the manuscript. MK and RK performed whole-slide image data acquisition. MN and KS collected some clinicopathological data from electrical records, graded and staged some cases, and reviewed the clinicopathological data which RS initially had collected, then corrected any incorrect data and filled in missing data. The final clinicopathological data were then verified by MN and KS to ensure the accuracy of the data. HI and HY performed histological diagnosis of carcinoma cases. RS and MS confirm the authenticity of all the raw data. All authors read and approved the final manuscript.

Ethics approval and consent to participate

This study was conducted after obtaining approval from Gunma University Ethical Review Board for Medical Research Involving Human Subjects (approval no. HS2024-068). Informed consent for this study was obtained by an opt-out method according to the 'Ethical Guidelines for Medical and Health Research Involving Human Subjects' established by Ministry of Education, Culture, Sports, Science and Technology and Ministry of Health, Labour and Welfare in Japan. Because the FFPE samples were used secondarily after their initial diagnostic purpose, we published a notification about this study on the Gunma University Hospital website instead of obtaining individual informed consent. The notice provided an outline of the research plan, details of the patient information to be used, the storage period and methods for the samples, contact information, and assurance of the right to freely withdraw from the study.

Patient consent for publication

Not applicable.

Competing interests

The authors declare that they have no competing interests.

References

1. Bray F, Laversanne M, Sung H, Ferlay J, Siegel RL, Soerjomataram I and Jemal A: Global cancer statistics 2022: GLOBOCAN estimates of incidence and mortality worldwide for 36 cancers in 185 countries. CA Cancer J Clin 74: 229-263, 2024.
2. Shuch B, Amin A, Armstrong AJ, Eble JN, Ficarra V, Lopez-Beltran A, Martignoni G, Rini BI and Kutikov A: Understanding pathologic variants of renal cell carcinoma: Distilling therapeutic opportunities from biologic complexity. Eur Urol 67: 85-97, 2015.
3. Sepp T, Poyhonen A, Uusküla A, Kotsar A, Veitonmäki T, Tammela TLJ, Baburin A and Murtola TJ: Renal cancer survival in clear cell renal cancer compared to other types of tumor histology: A population-based cohort study. PLoS One 20: e0329000, 2025.
4. Muglia VF and Prando A: Renal cell carcinoma: Histological classification and correlation with imaging findings. Radiol Bras 48: 166-174, 2015.
5. Montironi R, Santinelli A, Pomante R, Mazzucchelli R, Colanzi P, Filho AL and Scarpelli M: Morphometric index of adult renal cell carcinoma. Comparison with the Fuhrman grading system. Virchows Arch 437: 82-89, 2000.
6. Delahunt B, Srigley JR, Judge MJ, Amin MB, Billis A, Camparo P, Evans AJ, Fleming S, Griffiths DF, Lopez-Beltran A, *et al*: Data set for the reporting of carcinoma of renal tubular origin: recommendations from the international collaboration on cancer reporting (ICCR). Histopathology 74: 377-390, 2019.
7. Lang H, Lindner V, de Fromont M, Molinié V, Letourneux H, Meyer N, Martin M and Jacqmin D: Multicenter determination of optimal interobserver agreement using the Fuhrman grading system for renal cell carcinoma: Assessment of 241 patients with > 15-year follow-up. Cancer 103: 625-629, 2005.
8. Dagher J, Delahunt B, Rioux-Leclercq N, Egevad L, Srigley JR, Coughlin G, Dunglinson N, Gianduzzo T, Kua B, Malone G, *et al*: Clear cell renal cell carcinoma: Validation of World Health Organization/International Society of Urological Pathology grading. Histopathology 71: 918-925, 2017.
9. de las Heras JI and Schirmer EC: The nuclear envelope and cancer: A diagnostic perspective and historical overview. Adv Exp Med Biol 773: 5-26, 2014.

10. Nmezi B, Xu J, Fu R, Armiger TJ, Rodriguez-Bey G, Powell JS, Ma H, Sullivan M, Tu Y, Chen NY, *et al*: Concentric organization of A- and B-type lamins predicts their distinct roles in the spatial organization and stability of the nuclear lamina. Proc Natl Acad Sci USA 116: 4307-4315, 2019.
11. Vahabikashi A, Sivagurunathan S, Nicdao FAS, Han YL, Park CY, Kittisopikul M, Wong X, Tran JR, Gundersen GG, Reddy KL, *et al*: Nuclear lamin isoforms differentially contribute to LINC complex-dependent nucleocytoskeletal coupling and whole-cell mechanics. Proc Natl Acad Sci USA 119: e2121816119, 2022.
12. Moss SF, Krivosheyev V, de Souza A, Chin K, Gaetz HP, Chaudhary N, Worman HJ and Holt PR: Decreased and aberrant nuclear lamin expression in gastrointestinal tract neoplasms. Gut 45: 723-729, 1999.
13. Lammerding J, Hsiao J, Schulze PC, Kozlov S, Stewart CL and Lee RT: Abnormal nuclear shape and impaired mechanotransduction in emerin-deficient cells. J Cell Biol 170: 781-791, 2005.
14. Vaughan A, Alvarez-Reyes M, Bridger JM, Broers JL, Ramaekers FC, Wehnert M, Morris GE, Whitfield WGF and Hutchison CJ: Both emerin and lamin C depend on lamin A for localization at the nuclear envelope. J Cell Sci 114: 2577-2590, 2001.
15. Haque F, Mazzeo D, Patel JT, Smallwood DT, Ellis JA, Shanahan CM and Shackleton S: Mammalian SUN protein interaction networks at the inner nuclear membrane and their role in laminopathy disease processes. J Biol Chem 285: 3487-3498, 2010.
16. Ketema M, Wilhelmsen K, Kuikman I, Janssen H, Hodzic D and Sonnenberg A: Requirements for the localization of nesprin-3 at the nuclear envelope and its interaction with plectin. J Cell Sci 120: 3384-3394, 2007.
17. Banerjee I, Zhang J, Moore-Morris T, Pfeiffer E, Buchholz KS, Liu A, Ouyang K, Stroud MJ, Gerace L, Evans SM, *et al*: Targeted ablation of nesprin 1 and nesprin 2 from murine myocardium results in cardiomyopathy, altered nuclear morphology and inhibition of the biomechanical gene response. PLoS Genet 10: e1004114, 2014.
18. Heffler J, Shah PP, Robison P, Phyo S, Veliz K, Uchida K, Bogush A, Rhoades J, Jain R and Prosser BL: A balance between intermediate filaments and microtubules maintains nuclear architecture in the cardiomyocyte. Circ Res 126: e10-e26, 2020.
19. Xin H, Tang Y, Jin YH, Li HL, Tian Y, Yu C, Zhao ZJ, Wu MS and Pan YF: Knockdown of *LMNA* inhibits Akt/β-catenin-mediated cell invasion and migration in clear cell renal cell carcinoma cells. Cell Adh Migr 17: 1-14, 2023.
20. Radspieler MM, Schindeldecker M, Stenzel P, Forsch S, Tagscherer KE, Herpel E, Hohenfellner M, Hatiboglu G, Roth W and Macher-Goeppinger S: Lamin-B1 is a senescence-associated biomarker in clear-cell renal cell carcinoma. Oncol Lett 18: 2654-2660, 2019.
21. Fukushima T, Kobatake K, Miura K, Takemoto K, Yamanaka R, Tasaka R, Kohada Y, Miyamoto S, Sekino Y, Kitano H, *et al*: Nesprin1 deficiency is associated with poor prognosis of renal cell carcinoma and resistance to sunitinib treatment. Oncology 102: 868-879, 2024.
22. Lee S and Lee DK: What is the proper way to apply the multiple comparison test? Korean J Anesthesiol 71: 353-360, 2018.
23. Rosner B: Fisher's exact test. In: Fundamentals of Biostatistics. Cengage, Boston, pp387-394, 2019.
24. Lydersen S, Pradhan V, Senchaudhuri P and Laake P: Choice of test for association in small sample unordered r x c tables. Stat Med 26: 4328-4343, 2007.
25. Guilford JP: Correlation. In: Fundamental Statistics in Psychology and Education. McGraw-Hill Book Company, New York, pp 154-173, 1950.
26. Gospodarowicz M and Mason M: Kidney. In: TNM Classification of malignant tumours. O'Sullivan B, Mason M, Asamura H, *et al* (eds). Wiley Blackwell, Oxford, pp 199-203, 2017.
27. Capo-chichi CD, Aguida B, Chabi NW, Cai QK, Offrin G, Agossou VK, Sanni A and Xu XX: Lamin A/C deficiency is an independent risk factor for cervical cancer. Cell Oncol (Dordr) 39: 59-68, 2016.
28. Lammerding J, Fong LG, Ji JY, Reue K, Stewart CL, Young SG and Lee RT: Lamins A and C but not lamin B1 regulate nuclear mechanics. J Biol Chem 281: 25768-25780, 2006.
29. Pujadas Liwag EM, Wei X, Acosta N, Carter LM, Yang J, Almassalha LM, Jain S, Daneshkhah A, Rao SSP, Seker-Polat F, *et al*: Depletion of lamins B1 and B2 promotes chromatin mobility and induces differential gene expression by a mesoscale-motion-dependent mechanism. Genome Biol 25: 77, 2024.
30. Harborth J, Elbashir SM, Bechert K, Tuschl T and Weber K: Identification of essential genes in cultured mammalian cells using small interfering RNAs. J Cell Sci 114: 4557-4565, 2001.
31. Reis-Sobreiro M, Chen JF, Novitskaya T, You S, Morley S, Steadman K, Gill NK, Eskaros A, Rotinen M, Chu CY, *et al*: Emerin deregulation links nuclear shape instability to metastatic potential. Cancer Res 78: 6086-6097, 2018.
32. Stewart-Hutchinson PJ, Hale CM, Wirtz D and Hodzic D: Structural requirements for the assembly of LINC complexes and their function in cellular mechanical stiffness. Exp Cell Res 314: 1892-1905, 2008.
33. Lombardi ML, Jaalouk DE, Shanahan CM, Burke B, Roux KJ and Lammerding J: The interaction between nesprins and sun proteins at the nuclear envelope is critical for force transmission between the nucleus and cytoskeleton. J Biol Chem 286: 26743-26753, 2011.
34. Matsumoto A, Hieda M, Yokoyama Y, Nishioka Y, Yoshidome K, Tsujimoto M and Matsuura N: Global loss of a nuclear lamina component, lamin A/C, and LINC complex components SUN1, SUN2, and nesprin-2 in breast cancer. Cancer Med 4: 1547-1557, 2015.
35. Ueda N, Maekawa M, Matsui TS, Deguchi S, Takata T, Katahira J, Higashiyama S and Hieda M: Inner nuclear membrane protein, SUN1, is required for cytoskeletal force generation and focal adhesion maturation. Front Cell Dev Biol 10: 885859, 2022.
36. Östlund C, Folker ES, Choi JC, Gomes ER, Gundersen GG and Worman HJ: Dynamics and molecular interactions of linker of nucleoskeleton and cytoskeleton (LINC) complex proteins. J Cell Sci 122: 4099-4108, 2009.
37. Haque F, Lloyd DJ, Smallwood DT, Dent CL, Shanahan CM, Fry AM, Trembath RC and Shackleton S: SUN1 interacts with nuclear lamin A and cytoplasmic nesprins to provide a physical connection between the nuclear lamina and the cytoskeleton. Mol Cell Biol 26: 3738-3751, 2006.
38. Nishioka Y, Imaizumi H, Imada J, Katahira J, Matsuura N and Hieda M: SUN1 splice variants, SUN1_888, SUN1_785, and predominant SUN1_916, variably function in directional cell migration. Nucleus 7: 572-584, 2016.
39. Sharma VP, Williams J, Leung E, Sanders J, Eddy R, Castracane J, Oktay MH, Entenberg D and Condeelis JS: SUN-MKL1 crosstalk regulates nuclear deformation and fast motility of breast carcinoma cells in fibrillar ECM microenvironment. Cells 10: 1549, 2021.
40. Mislow JM, Holaska JM, Kim MS, Lee KK, Segura-Totten M, Wilson KL and McNally EM: Nesprin-1alpha self-associates and binds directly to emerin and lamin A in vitro. FEBS Lett 525: 135-140, 2002.
41. Duong NT, Morris GE, Lam le T, Zhang Q, Sewry CA, Shanahan CM and Holt I: Nesprins: Tissue-specific expression of epsilon and other short isoforms. PLoS One 9: e94380, 2014.
42. Sur-Erdem I, Hussain MS, Asif M, Pinarbasi N, Aksu AC and Noegel AA: Nesprin-1 impact on tumorigenic cell phenotypes. Mol Biol Rep 47: 921-934, 2020.
43. Wilhelmsen K, Litjens SH, Kuikman I, Tshimbalanga N, Janssen H, van den Bout I, Raymond K and Sonnenberg A: Nesprin-3, a novel outer nuclear membrane protein, associates with the cytoskeletal linker protein plectin. J Cell Biol 171: 799-810, 2005.
44. Morgan JT, Pfeiffer ER, Thirkill TL, Kumar P, Peng G, Fridolfsson HN, Douglas GC, Starr DA and Barakat AI: Nesprin-3 regulates endothelial cell morphology, perinuclear cytoskeletal architecture, and flow-induced polarization. Mol Biol Cell 22: 4324-4334, 2011.
45. Diegmiller R, Doherty CA, Stern T, Imran Alsous J and Shvartsman SY: Size scaling in collective cell growth. Development 148: dev199663, 2021.
46. Chiarini F, Paganelli F, Balestra T, Capanni C, Fazio A, Manara MC, Landuzzi L, Petrini S, Evangelisti C, Lollini PL, *et al*: Lamin A and the LINC complex act as potential tumor suppressors in ewing sarcoma. Cell Death Dis 13: 346, 2022.
47. Lv XB, Liu L, Cheng C, Yu B, Xiong L, Hu K, Tang J, Zeng L and Sang Y: SUN2 exerts tumor suppressor functions by suppressing the warburg effect in lung cancer. Sci Rep 5: 17940, 2015.